

Ultrasonic light storage in a quantum well: A photon assembly line

A. Wixforth^{a,*}, C. Rocke^a, S. Zimmermann^a, J.P. Kotthaus^a, G. Böhm^b, G. Weimann^{1b}

^a *Sektion Physik der LMU, Geschwister-Scholl-Platz 1, D-80539 München, Germany*

^b *Walter-Schottky-Institut der TU München, Coulombwall 1, D-85748 Garching, Germany*

Abstract

Surface acoustic waves are used to effectively convert photogenerated excitons in a piezoelectric semiconductor quantum well into long-lived electron–hole polarizations. The strong lateral piezoelectric fields ionize the excitons and spatially separate the resulting electrons and holes. The strongly reduced wave function overlap results in very long storage times for this polarization which propagates across the sample at the speed of sound. External and deliberate screening of the piezoelectric fields triggers radiative recombination after long delay times and at a remote location of the sample.

PACS: 73.50.Rb.; 77.65.Dq.; 78.20.Hp.; 78.55.Cr

Keywords: Surface acoustic waves; Excitons; Quantum well; Photon conveyor belt

The optoelectronic properties of band-gap-engineered semiconductor structures have attracted tremendous interest over the last decade or so. Great interest in optical computing and the need for fast telecommunication techniques have triggered the development of various devices for modulation, detection, and all-optical switching [1]. Many of the above devices, based on layered, band-gap-engineered semiconductor structures make use of the fact that strong electric fields modify the optical properties [2]. For example, an electric field applied perpendicular to a quantum well

(QW) results in the so-called quantum confined Stark effect (QCSE) [3]. Here, the energies for interband transitions are red-shifted with respect to the unperturbed case. On the other hand, *vertical* doping superlattices have been employed to reduce the effective band gap due to spatially indirect transitions by an amount that can be tuned by voltages between the n- and p-doped layers [4]. The strength of the interband transitions under consideration, however, is dominated largely by the atomic-like Bloch parts of the wave functions involved [5]. Thus, it appears to be unavoidable that strong interband optical transitions are linked to direct band gap semiconductors with short radiative lifetimes such as GaAs, whereas long radiative lifetimes of photogenerated carriers imply the use of semiconductors with indirect band gaps such as Si and correspondingly reduced interband

*Corresponding author. Tel.: + 49 89 2180 3732; fax: + 49 89 2180 3182; e-mail: achim.wixforth@physik.uni-muenchen.de

¹ Now at: Fraunhofer Institut IAF, Tullastrasse, D-79108 Freiburg, Germany.

absorption. In modulation-doped superlattices, this problem has been tackled by a combination of a direct gap in momentum space with an indirect gap in real space. Here, the spatial separation of photogenerated electrons and holes leads to considerably prolonged lifetimes together with strong interband absorption [6]. Earlier attempts to follow this route for *lateral* superlattices showed that also electric fields parallel to the plane of a quantum well may result in very attractive tuneable optical properties [7]. It could be shown, for instance, that field ionization of excitons in the plane of the well is also possible. Hence, a spatial electron–hole separation in the plane of the well may be achieved, which again results in very long life- or storage times of the optical excitations [8].

Here, we demonstrate a completely new way of combining large interband absorption with very long lifetimes of the photoexcited polarizations. Moreover, the lateral potential modulation in our case is of dynamical nature which propagates across the sample at the speed of sound [9]. To create a lateral superlattice with the above features, we use surface acoustic waves (SAW) [10], which – provided they propagate on a piezoelectric substrate – are accompanied by strong piezoelectric fields and potentials. It has been shown before that the piezofields of a SAW can effectively couple to quasi-two-dimensional mobile carriers in the semiconductor, a fact that has been employed to study the dynamic conductivity of these carriers [11,12].

We show that the confinement of photogenerated electron–hole (e–h) pairs to two dimensions together with the moving lateral superlattice allows reversible charge separation [13]. We demonstrate that the combination of both the advantages of strong interband absorption and extremely long lifetimes of the optical excitations is achieved without affecting the superior optical quality of the quantum well material. The piezoelectric fields of the SAW can be strong enough to field-ionize optically generated excitons and to confine the resulting electrons and holes in the moving lateral potential wells separated by one-half wavelength of the SAW. The spatial separation dramatically reduces the recombination probability and increases the radiative lifetime by several orders of

magnitude as compared to the unperturbed case. We further demonstrate that the dynamically trapped electron–hole pairs can be transported over macroscopic distances at the speed of sound and that deliberate screening of the lateral piezoelectric fields of the SAW leads to an induced radiative recombination after long storage times at a location remote from the one of e–h generation. This conversion and consequent slowing down of photons into a long-lived electron–hole polarization which is efficiently reconverted into photons can be regarded as an optical delay line operating at sound velocities.

SAW are modes of elastic energy that propagate at the free surface of a solid and decay typically over a wavelength with depth into the material. The particle displacement in a SAW is elliptical, leading to both lateral and vertical electric fields that oscillate both in space and time. For a (1 0 0)-GaAs surface, the [1 1 0] and equivalent directions are piezoactive directions with appreciable electromechanical coupling coefficients [11]. The SAW velocity in this case is $v_{\text{SAW}} = 2865$ m/s. SAW are usually excited by means of so-called interdigital transducers (IDT), two comb-like metallic structures the design of which largely governs the frequency response of the sample. Usually, one emitting and one receiving IDT are used to create a SAW delay line. The center frequency of such a delay line is given by $f_{\text{SAW}} = v_{\text{SAW}}/\lambda_{\text{SAW}}$, the wavelength λ_{SAW} being determined by the period of the IDT.

The undoped quantum well samples used in our experiments are grown by molecular beam epitaxy on a (1 0 0)-GaAs substrate. The well consists of 10 nm pseudomorphic $\text{In}_{0.15}\text{Ga}_{0.85}\text{As}$ grown on a 1 μm thick GaAs buffer and is covered by a 20 nm thick GaAs cap layer. The active area of the sample is etched into a 2.5 mm long and 0.3 mm wide mesa (see inset of Fig. 1) with two IDTs at its ends. The IDTs are designed to operate at a center frequency $f_{\text{SAW}} = 840$ MHz. They are partially impedance matched to the 50 Ω radio frequency (RF) circuitry using an on-chip matching network thus strongly reducing the insertion loss of each transducer. Our sample is mounted in an optical cryostat and the experiments presented here are performed at $T = 4.2$ K. Light from a pulsed laser diode ($\lambda_{\text{laser}} = 780$ nm) is used for optical interband

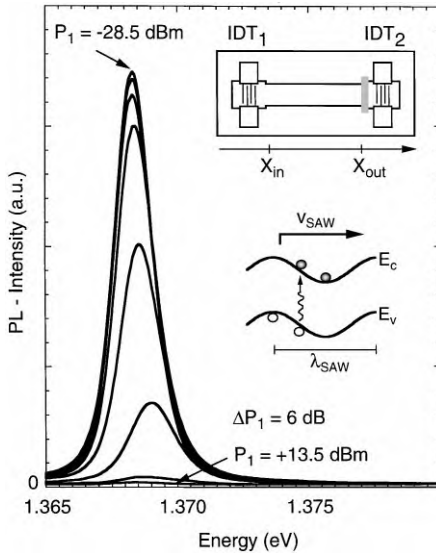


Fig. 1. PL spectra of a single 10 nm wide InGaAs/GaAs quantum well structure for different acoustic powers of the SAW. The optical excitation occurs at the center of the mesa with a laser intensity of 10 mW/cm^2 and wavelength $\lambda_{\text{laser}} = 780 \text{ nm}$. The inset schematically depicts the sample with an etched mesa and two interdigital transducers. Field ionization and subsequent storage of the photogenerated carriers in the moving lateral potential is also sketched [9].

excitation above band gap and the photoluminescence (PL) of the sample is analysed in a triple grating spectrometer. Either a photomultiplier or a charged coupled device (CCD) serve as a detector for the PL. Application of a high-frequency signal to one of the IDT launches a SAW that can be detected at the other IDT after the acoustic delay of order of $1 \mu\text{s}$ determined by the spacing of the IDTs. Either pulsed or continuous wave (cw) operation of the SAW transducers is possible.

In Fig. 1, we show a set of PL spectra taken for different SAW intensities on the sample. Laser illumination and detection of the PL is done at the same spot of the sample, close to the mesa center. The observed PL in this case is referred to as the ‘direct’ PL, in the sense that it is local and instantaneous, in contrast to the ‘delayed’ PL that we will address below. With increasing SAW amplitude (given in dBm) we observe a strong decrease of the PL intensity, until at the highest power used ($+13.5 \text{ dBm} = 22.4 \text{ mW}$) the PL is completely

suppressed. At the same time we observe a slight shift of the PL line towards higher energy, a fact that can be associated to the acoustically induced lateral Franz–Keldysh effect [7].

The piezoelectric fields of the SAW modulate the band edges with respect to the chemical potential similar as in doping superlattices [4] or statically imposed laterally periodic electric fields using an interdigitated gate electrode [7]. In our moving potential superlattice with period $\lambda = 3.4 \mu\text{m}$ the excitons become polarized predominantly by the lateral electric field until they dissociate at high fields into spatially separated e - h pairs. These are then efficiently stored in the potential minima and maxima of the conduction and the valence band, respectively (inset of Fig. 1). For an acoustic power of $P_1 = +13.5 \text{ dBm}$ lateral fields as high as $E_{\text{lat}} = 8 \text{ kV/cm}$ and vertical fields up to $E_{\text{vert}} = 10 \text{ kV/cm}$ are achieved [14] (see Fig. 2). A very simple estimate yields that fields as high as $E_{\text{crit}} \approx E_b/(ea_B^*) \sim 10^4 \text{ V/cm}$ will ionize photogenerated excitons. $E_b \sim 9 \text{ meV}$ denotes the exciton binding energy, e the elementary charge, and $a_B^* \sim 9 \text{ nm}$ the effective (Bohr) exciton radius of our system. Hence, the lateral field of the SAW should be high enough to dissociate the photogenerated excitons in our sample. The influence of the vertical fields, however, can be neglected in our case as we are working on a comparatively thin ($d = 10 \text{ nm}$) quantum well.

This quenching of the PL under the influence of an intense SAW is already an indication of the increased trapping probability in the moving lateral potential of the SAW. As the potential modulation is moving with speed of sound, consequently, the spatially separated and trapped e - h pairs are swept away by the SAW and propagated across the sample without recombining. The dramatically prolonged recombination time together with their propagation along the surface of the quantum well enables us to directly follow the transport of photogenerated carriers over macroscopic distances that may exceed millimeters in our experiment.

In Fig. 3, we depict the result of such an experiment. The inset schematically shows the dynamics involved. At $t = 0$, a SAW is excited by feeding a radio-frequency pulse ($f = 840 \text{ MHz}$, $\tau = 200 \text{ ns}$) onto the IDT. At $t = t_1$, some 200 ns after excitation,

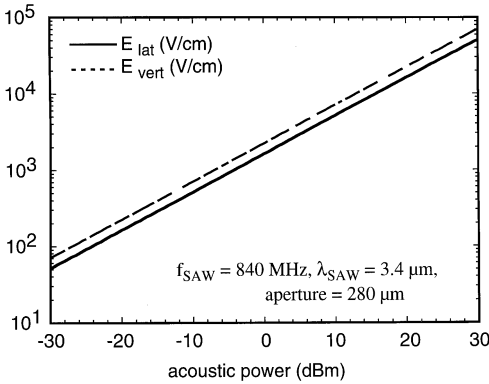


Fig. 2. Calculated piezoelectric lateral and vertical fields of the SAW as a function of the acoustic power for the sample used in our experiment.

the SAW pulse arrives at $x = x_{in}$, where we focus the light of a pulsed laser on the sample. We photogenerate excitons, which are immediately dissociated in the strong lateral field of the SAW at $x = x_{in}$. This dissociation is indirectly observed by a clear reduction of the parasitic stray light at the detector coming from the ‘direct’ PL at $x = x_{in}$. Consequently, the electron–hole pairs are trapped in their respective energetic minima, i.e. the electrons in the potential minima of the SAW, and the holes in the valence band maxima. There, the electrons and holes are separated from each other by about half an acoustical wavelength ($\lambda_{SAW}/2$) = 1.7 μm . As pointed out above, this reduces the wave function overlap and efficiently inhibits radiative recombination. Shortly after ‘loading’ the moving potential wells of the SAW, the laser diode is switched off. In terms of their natural recombination time $\tau_{rec} \sim 1$ ns the stripes of electrons and holes now travel ‘forever’, surfing on the SAW like on a conveyor belt, until they reach the point $x = x_{out}$, where the lateral piezoelectric fields of the SAW are screened by a thin, semitransparent NiCr layer on top of the sample. Here, the photogenerated electrons and holes are again free to diffuse which results in a dramatically increased recombination probability and results in a reassembled flash of light at $t = t_2$, as observed by the detector. Only the length of the sound path between $x = x_{in}$ and $x = x_{out}$, $\Delta x = 1.0$ mm in this case, determines the storage

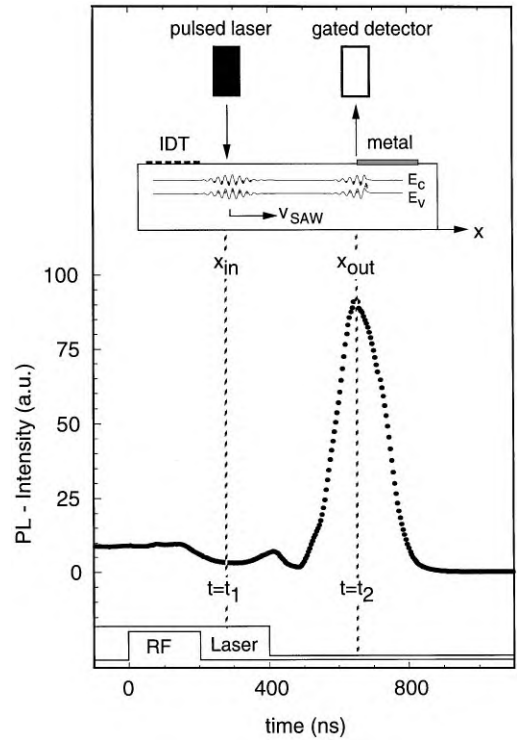


Fig. 3. Acoustically driven transport of ambipolar charges in the lateral electric field of a SAW. At $t = 0$, a 200 ns long RF pulse at $f_{SAW} = 840$ MHz applied to IDT₁ generates a SAW with an acoustic power of $P_1 = 13.5$ dB m. At $t = t_1$ and $x = x_{in}$ the potential extrema of the SAW are filled with photogenerated e–h pairs which are transported with sound velocity to a semitransparent metallization at $x = x_{out}$. Here the deliberate screening of the piezoelectric potential modulation lifts the spatial separation of the carriers and induces radiative recombination at $x = x_{out}$ and $t = t_2$. The duration of the RF pulse and the laser pulse are indicated in the lower part [9].

time that has been achieved in the present experiment. Comparing the intensity of the ‘delayed’ PL to the ‘direct’ one shows that only a small fraction of the photogenerated carriers are ‘lost’ along their way. This loss is mainly caused by non-radiative recombination at the mesa edges or wavefront inhomogeneities of the SAW and can be reduced by a proper design of future samples.

The threshold behavior of the field ionization of the photogenerated excitons and the transport of their fragments (e–h pairs) can be clearly seen in Fig. 4. Here, we depict the normalized PL

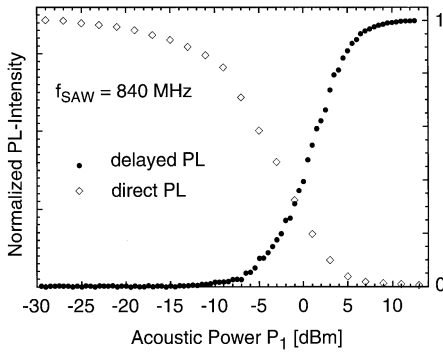


Fig. 4. Normalized direct and delayed PL intensities as a function of the acoustic power P_1 . Efficient ambipolar transport of charges resulting in a time-delayed PL signal requires a minimum threshold acoustic power of $P_1 = -5$ dB m which corresponds to a minimum lateral electric field strength $E_{\text{lat}} = 2$ kV/cm. This threshold coincides with the quenching of the direct PL signal [9].

intensities of both the ‘direct’ and instantaneous PL at $x = x_{\text{in}}$ together with the one of the ‘delayed’ PL as a function of the acoustic power in the SAW. As already seen in Fig. 1, with increasing SAW power the direct PL intensity reduces and finally quenches at the highest powers shown. At the same time the observed delayed PL intensity at site $x = x_{\text{out}}$ strongly increases. The power necessary for efficient ionization and subsequent transport corresponds well with the estimated critical lateral field strength of $F_{\text{crit}} \sim 10^4$ V/cm.

We just showed that the screening of the lateral piezoelectric fields of a SAW by external means triggers radiative recombination of the travelling e–h pairs by reassembling them into photons. Another way of doing so is to use a second, counter-propagating SAW to result in a standing wave interference pattern, when both SAW collide. To achieve this, it is necessary that both SAW have the same amplitude and frequency. In Fig. 5, we show the result of this alternative experiment for a reassembly of the e–h-pairs on the photon conveyor belt: Adjusting the amplitude of a first SAW (say the one launched at IDT1) such that the direct PL is partially quenched, we varied the amplitude of a second, counterpropagating SAW at the same frequency $f_1 = f_2 = 840$ MHz. The PL in this case is monitored by the detector at the point of

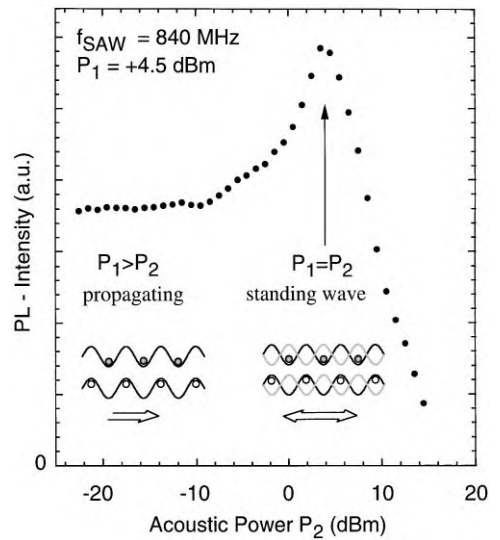


Fig. 5. Direct PL intensity at the center of the sound path as a function of the acoustic power P_2 for a constant acoustic power $P_1 = +4.5$ dB m. For the standing wave geometry at $P_1 = P_2$ the spatial separation between electrons and holes is lifted resulting in a recovered PL intensity due to the increased transition probability [9].

collision of the two SAW, close to the center of the mesa. At low power levels P_2 , the counter-propagating SAW₂ is just a small perturbation to the original SAW₁, and the PL intensity remains nearly unchanged. With increasing P_2 , however, the interference of both SAW lead to a standing wave situation, where the time averaged wave function overlap of the trapped e–h-pairs becomes finite. This increases the recombination probability which results in a strong increase of the observed PL and a maximum at $P_1 = P_2 = +4.5$ dB m in this case. Further increase of P_2 reverses the situation: Now SAW₂ takes over the charges, the PL quenches and the direction of flow is reversed as compared to the beginning of the experiment. In this experiment it is demonstrated that the time and the location of radiative recombination of the stored and trapped charges in a SAW can be chosen at will, simply by adjusting the time delay between the launch of the two SAW pulses. We could also show that stored and trapped charges can be taken over by a SAW pulse that propagates perpendicularly to the original wave. This way,

optical information may be transferred across the sample in two dimensions, which may be used to multiplex an optical input signal to different output ports, like on a switchboard.

Finally, it should be mentioned that the energy of the ‘delayed’ PL needs not necessarily to be the same as the one of the ‘direct’ PL. Local modifications of the quantum well or material properties at the site of recombination results in a different PL energy at this location. For instance, local stressors, local changes of the bandgap by interdiffusion, or locally applied electric fields by means of gate electrodes on top of the quantum well surface may result in a change of the effective bandgap and thus the energy of the delayed PL. As the SAW can be used to steer the trapped and stored carriers to different locations of the sample plane, the delayed PL can be tuned in most any desired fashion. One can also imagine to use our photon conveyor belt to pump an optically active structure like a laser structure on the same chip. This way, even very sophisticated signal processing or amplification of the optical input would be possible.

In summary, we have shown that the strong piezoelectric fields in a surface acoustic wave can be used to efficiently transform photons into electron–hole polarizations that travel across a semiconductor quantum well at more leisure pace. The lateral fields in the SAW dissociate optically generated excitons into lateral and spatially separated stripes of electrons and holes, like on a conveyor belt or an assembly line. This spatial separation dramatically increases the radiative life times, an increase by about a factor of thousand has already been demonstrated. The moving lateral potential of the SAW is furthermore able to transport the stored e–h-pairs to a location of the sample that is remote from the one of their creation. We have shown that external and deliberate screening of the lateral piezoelectric fields triggers radiative recombination in form of a ‘delayed’ PL at the remote site. Screening of the SAW fields can be achieved by many different means, two of which – metallization and standing wave geometry – we have discussed in detail.

We gratefully acknowledge many fruitful discussions with A.O. Govorov, and M. Rotter. Many of the experiments would not have been possible without the excellent technical support of S. Manus. This work has been sponsored by the Deutsche Forschungsgemeinschaft (DFG), and by the Bayerische Forschungsförderung FOROPTO.

References

- [1] See, e.g., The special issues on Smart Pixels [IEEE J. Quantum Electron. 29 (2), (1993), Spatial Light Modulators [Appl. Opt. 31(20), 1992, and Optical Computing [Appl. Opt. 31(26), 1992.
- [2] D.A.B. Miller, Opt. Quantum Electron. 22 (1990) S61.
- [3] D.A.B. Miller, D.S. Chemla, T.C. Damen, A.C. Gossard, W. Wiegmann, T.H. Wood, C.A. Burrus, Phys. Rev. Lett. 53 (1984) 2173.
- [4] G.H. Döhler, H. Künzel, D. Olego, K. Ploog, P. Ruden, H.J. Stolz, G. Abstreiter, Phys. Rev. Lett. 47 (1981) 864.
- [5] See, e.g., C. Weisbuch, B. Vinter, Quantum Semiconductor Structures, Academic Press, San Diego, 1991.
- [6] G.H. Döhler, G. Hasnain, J.N. Miller, Appl. Phys. Lett. 49 (1986) 704.
- [7] A. Schmeller, W. Hansen, J.P. Kotthaus, G. Tränkle, G. Weimann, Appl. Phys. Lett. 64 (1994) 330.
- [8] S. Zimmermann, A.O. Govorov, W. Hansen, J.P. Kotthaus, C. Rocke, A. Wixforth, M. Bichler, W. Wegscheider, in these Proceedings (MSS8), Physica E 2 (1998).
- [9] C. Rocke, S. Zimmermann, A. Wixforth, J.P. Kotthaus, G. Böhm, G. Weimann, Phys. Rev. Lett. 78 (1997) 4099.
- [10] Interestingly, one of the earliest proposals to create a semiconductor superlattice was to use sound waves: L.V. Keldysh, Sov. Phys. Solid State 4 (1962) 1658.
- [11] A. Wixforth, J. P. Kotthaus, G. Weimann, Phys. Rev. Lett. 56 (1986) 2104. A. Wixforth, M. Wassermeier, J. Scriba, J.P. Kotthaus, G. Weimann, W. Schlapp, Phys. Rev. B 40 (1989) 7874.
- [12] R.L. Willet, R.R. Ruel, K.W. West, L.N. Pfeiffer, Phys. Rev. Lett. 71 (1993) 3846.
- [13] Transport of unipolar charges in epitaxial films is usually referred to as acoustic charge transport (ACT), see e.g. M.J. Hoskins, B.J. Hunsinger, Appl. Phys. Lett. 41 (1982) 332; W.J. Tanski, S.W. Merritt, R.N. Sacks, D.E. Cullen, E.J. Branciforte, R.D. Carroll, T.C. Eschrich, Appl. Phys. Lett. 52 (1988) 18.
- [14] J.F. Jain, K.K. Bhattacharjee, IEEE Photonics Technol. Lett. 1 (1989) 307.